Tumor Recovery by Angiogenic Switch from Sprouting to Intussusceptive Angiogenesis after Treatment with PTK787/ZK222584 or Ionizing Radiation

Ruslan Hlushchuk,*¶ Oliver Riesterer,† Oliver Baum,* Jeanette Wood,‡ Guenther Gruber,§ Martin Pruschy,† and Valentin Djonov*¶

From the Institute of Anatomy, University of Bern, Bern, Switzerland; Department of Radiation Oncology,† University Hospital, Zurich, Switzerland; Novartis Pharma AG,‡ Basel, Switzerland; Department of Radiation Oncology,§ University Hospital, Bern, Switzerland; Institute of Anatomy,¶ University of Fribourg, Fribourg, Switzerland*

Inhibitors of angiogenesis and radiation induce compensatory changes in the tumor vasculature both during and after treatment cessation. To assess the responses to irradiation and vascular endothelial growth factor-receptor tyrosine kinase inhibition (by the vascular endothelial growth factor tyrosine kinase inhibitor PTK787/ZK222854), mammary carcinoma allografts were investigated by vascular casting; electron, light, and confocal microscopy; and immunoblotting. Irradiation and anti-angiogenic therapy had similar effects on the tumor vasculature. Both treatments reduced tumor vascularization, particularly in the tumor medulla. After cessation of therapy, the tumor vasculature expanded predominantly by intussusception with a plexus composed of enlarged sinusoidal-like vessels containing multiple transluminal tissue pillars. Tumor revascularization originated from preserved α-smooth muscle actin-positive vessels in the tumor cortex. Quantification revealed that recovery was characterized by an angiogenic switch from sprouting to intussusception. Up-regulated α-smooth muscle actin-expression during recovery reflected the recruitment of α-smooth muscle actin-positive cells for intussusception as part of the angio-adaptive mechanism. Tumor recovery was associated with a dramatic decrease (by 30% to 40%) in the intratumoral microvascular density, probably as a result of intussusceptive pruning and, surprisingly, with only a minimal reduction of the total microvascular (exchange) area. Therefore, the vascular supply to the tumor was not severely compromised, as demonstrated by hypoxia-inducible factor-1α expression. Both irradiation and anti-angiogenic therapy cause a switch from sprouting to intussusceptive angiogenesis, representing an escape mechanism and accounting for the development of resistance, as well as rapid recovery, after cessation of therapy.

Tumor relapse and the development of drug resistance is a major problem in the management of solid tumors. It may be inherent to the tumor-cell compartment, to the aberrant and inefficient vasculature, or to the surrounding stroma. In the first case, a refractory subpopulation of clonogenic cancer cells survives and proliferates. In the second case, the potency of therapy is hampered due to limited tumor perfusion. The tumor vasculature can be damaged by chemotherapeutics, but interestingly, in particular in response to inhibitors of angiogenesis, the tumor vasculature may undergo morphological changes that normalize the tumor vasculature. This tumor vascular normalization concept claims that treatment with low doses of angiogenesis inhibitors preferentially targets immature vessels and thereby creates a normalization of the blood vessel with improved functionality and results in better perfusion of the remaining tumor mass.[1] This could diminish tumor hypoxia by improved delivery of oxygen and also improve the delivery of chemotherapeutics.

The administration of anti-angiogenic agents is now generally recognized as a promising therapeutic approach in

Supported by the grant No3100A0-116243 from the Swiss National Science Foundation.

R. H. and O. R. contributed equally.

Address reprint requests to Valentin Djonov, MD, Rte A. Gockel 1, Institute of Anatomy, University of Fribourg, CH-1700 Fribourg, Switzerland. E-mail: valentin.djonov@unifr.ch.

the management of cancer patients.[2–5] During the past few years, many such drugs have been developed to target various steps in pathological vascularization, including cytokine-induced stimulation and integrin-mediated migration of vascular endothelial cells and enzymatic degradation of extracellular matrix components.[6,7]

Vascular endothelial growth factor (VEGF) is an extremely potent pro-angiogenic factor, which is involved in both physiological and pathological vascular growth. Many human neoplasms and animal tumor models express high mRNA and protein levels of VEGF.[2,8,9] Inhibition of VEGF or of its receptors should block the downstream cascade and interfere with its pro-angiogenic effects and thereby block tumor vascularization.

Bevacizumab, a humanized monoclonal antibody against VEGF, has validated this therapeutic approach in patients with various types of cancers. Its application, either alone or in combination with chemotherapy, has led to a significant increase in the survival rate of patients with metastatic colorectal cancer and other cancers.[10–12]

An alternative therapeutic strategy involves the suppression of VEGF signaling pathways. Indeed, tyrosine-kinase inhibitors of the VEGF receptors have been recently used as anti-angiogenic agents against pathological neovascularization and have even undergone early clinical evaluation.[13,14] Most of the agents, for example, Bay-43–9006 (Nexavar) or SU11248 (Sutent) are broad spectrum tyrosine-kinase inhibitors. PTK787/ZK22854 (PTK/ZK) (Vatalanib) (Novartis Pharma AG, Basel, Switzerland) is one of the most selective inhibitors of VEGFR-1, VEGFR-2, and VEGFR-3, which can be administered orally. Its dose-dependent anti-angiogenic effects and efficacy have been well documented, both in animal models and in human patients.[15–19]

Treatment response to radiotherapy is partly determined by sensitivity of the tumor vasculature to radiation. Studies show that endothelial apoptosis determines radiation response in murine tumor models.[20,21] In addition clinical studies show that an angiogenic response, as indicated by changes in microvessel density after radiotherapy, significantly correlate with response to radiation and survival.[22,23] A reduction in tumor vascularization would be expected to increase resistance of tumor cells to irradiation since tumor cells irradiated in normoxic conditions are 2 to 3 times more radiosensitive than cells irradiated under severe hypoxia. However, anti-VEGF/VEGFR strategies enhance, rather than reduce the effects of fractionated radiation.[24] Tumor re-oxygenation as part of vascular response to anti-angiogenic therapy could be a mechanism of the increased sensitivity of tumors to ionizing radiation after anti-angiogenic therapy. Thus it is important to understand morphological changes of the tumor vasculature after either radio or anti-angiogenic therapy in more detail.

Vascular morphological alterations by means of intussusceptive angiogenesis have been observed in hepatocellular carcinoma model during treatment with sirolimus, a mTOR inhibitor.[25] Treated rats had significantly longer survival, developed smaller tumors and fewer extrahepatic metastases. During the treatment and during the early recovery phase vascular sprouting was absent, whereas intussusception was observed. Intussusceptive angiogenesis has been extensively described in the last decade during normal development and growth [for more details see reviews[26,27]]. Intussusception, ie, the formation of transluminal tissue pillars, represents an alternative to the sprouting mode of angiogenesis. It is an important mechanism of capillary growth, formation of small arteries and veins, vascular pruning and angio-adaptive remodeling. Intussusception is associated with alterations in hemodynamic conditions and acts only in preexisting vasculature.

The advantages of this latter mechanism of growth over sprouting are that: (i) blood vessels are generated more rapidly; (ii) it is energetically and metabolically more economic, since extensive proliferation of endothelial cells, degradation of the basement membrane and invasion of the surrounding tissue are probably not required; and (iii) the capillaries thereby formed are less leaky.[26,27] Vascular growth and remodeling by intussusception occur without disrupting of the organ function, which is essential during both embryonic development and postnatal life.

In the present study, we investigated the adaptive response of the tumor vasculature to a highly selective inhibitor of angiogenesis and to ionizing radiation and identified an angiogenic switch from sprouting to intussusceptive angiogenesis as novel mechanism to counteract the antivascular effects of both of these treatment modalities.

Materials and Methods

Tumor Xenografts in Nude Mice and the Administration of PTK/ZK or Radiotherapy

MMTV/c-neu murine carcinoma cells (4×10^6) were injected subcutaneously into the flank of 4- to 8-week-old athymic nude mice. Tumor volumes were determined from caliper measurements of tumor length (L) and width (l) according to the formula $(L \times l^2)/2$. Tumors were allowed to expand to a volume of minimally 200 mm^3 (diameter >7 mm) before treatment. Measurement of "volume Tu necrosis/entire Tu volume" ratio has been performed according to the Cavalieri's principle.[28] PTK787/ZK222584 (dissolved in water containing 5% dimethyl sulfoxide and 1% Tween-80) was administered orally at a dose of 100 mg/kg of body weight on 4 consecutive days. Mice subjected to radiotherapy received a daily dose of 3 Gy, likewise for 4 consecutive days. The tumors from control and both treated groups (altogether $n = 90$: $n = 6$ to 8 per time point and per group) were harvested on days 5, 9, 14, and 19 after the onset of treatment: 3 to 4 tumors for vascular casts and another 3 to 4 for paraffin and transmission electron microscopy sections and immunoblotting. All numerical data were statistically analyzed using the Mann-Whitney U-test. The animal experiments were conducted in accord with UKCCCR guidelines.[29]

α-Smooth Muscle Actin Immunoblotting

After solubilizing the tissue, 50-μg aliquots of the protein extracts were subjected to SDS-polyacrylamide gel electrophoresis on 10% gels under reducing conditions. The gels were transferred to nitrocellulose membranes (Schleicher and Schuell, Dassel, Germany) and treated with 5% (w/v) milk powder. They were then incubated overnight with antibodies specific for α-smooth muscle actin (SMA) [(Sigma, Buchs, Switzerland) diluted 1:5000]. Thereafter, they were treated for one hour with the corresponding peroxidase-conjugated secondary antibody (Sigma, Buchs, Switzerland). Bound antibodies were detected by chemoluminescence using an enhanced chemiluminescence detection kit (Supersignal, Pierce, Rockford, IL).

Vascular Casting, Morphology, and Morphometric Analysis

Vascular casts were prepared as previously described.[30] Briefly, the systemic or local vasculature was perfused with a freshly prepared solution of Mercox (Vilene Company, Japan) containing 0.1 ml of accelerator per 5 ml of resin. One hour after perfusion, the tumors were excised and transferred to 7.5% potassium hydroxide for the dissolution of tissue, which was effected over a course of 3 to 4 weeks.

For the further morphometric analysis the vascular casts were then frozen in water and bisected through the tumor center. Thereafter the casts were dried and glued onto aluminum stabs, sputtered with gold, and examined in a Philips XL-30 FEG scanning electron microscope. The positions for the quantitative evaluation (at least 10 per sample) were chosen using systematic uniform random sampling scheme.[31] Using this random technique there were some partially or almost "empty" fields corresponding to the necrotic areas in the tumor. Such fields have not been excluded from the analysis, but this was the reason why we have used such a parameter as numerical density per vessel area but not per field of view. This allowed us to consider all of the fields regardless of the grade of their "emptiness." Pillars were identified as holes in vascular casts whose diameter roughly measured less or equal to 2.5 μm. All holes greater than 2.5 μm normally referred to as meshes were ignored. Capillary sprouts were identified as tapered blind ending capillary branches without visible cut surface at its end and whose average diameter was less than 4 μm. The quantification technique used here has been described in detail by Makanya et al.[32]

Immunostaining for CD31 and SMA and Its Evaluation

For immunohistochemical evaluation 3-μm-thick paraffin sections of the tumors were processed according to Makanya et al.[32] The first antibodies diluted in Tris-buffered saline: mouse anti-CD31, diluted 1:20 (M-0823, clone JC/70A; Dako, Glostrup, Denmark); and mouse anti-SMA, diluted 1:200 (Sigma, Buchs, Switzerland). The analySIS Software 3.2 (Soft Imaging System, Munich, Germany) was used for estimation of intratumoral microvascular density and vascular area density. The pictures used for quantification were taken from vascular "hot spots" at $\times$200 magnification (at least four "hot spots" per tumor): after the inspection of a CD31-stained section through the tumor center the investigator picked up and took images of 6 to 8 fields of view with seemingly highest number of vessels. Afterward, the number of vessels was determined in each of the taken images and the four with the highest vessel count were considered for further analysis. If more than one image had the fourth highest vessel count, all of the images with this count were also considered for further analysis. The number of vessels per field of view was counted by the investigator by pointing (clicking) at each individual vessel in the images obtained and the mentioned software simply counted the number of "points." The vascular area density was calculated by overlaying the grid with 96 crossings points over the image. The number of crossing points that appeared to lie over the vessels was counted in the similar way as number of vessels (investigator-driven). The ratio between the obtained number and the total number of points in the overlay grid was the vessel area density.

Laser Scanning Microscopy and CD31-SMA Double Immunostaining

Sixty-μm-thick paraffin sections were pretreated according to Makanya et al.[32] In a second step they were incubated with the first antibody anti-CD31 (CD31 MEC13.3 [rat]), diluted 1:100 in Tris-buffered saline, then washed and incubated with mouse anti-SMA, diluted 1:200 (Sigma, Buchs, Switzerland). Sections were exposed to a second goat anti-rat antibody coupled with CyTM3 (Jackson ImmunoResearch Laboratories, Inc., PA) diluted 1:200 in Tris-buffered saline for 60 minutes at ambient temperature, washed, and then incubated with anti-mouse antibody coupled with fluorescein isothiocyanate for a similar period at the same temperature. The sections were then washed, mounted with Mowiol, and examined using a Zeiss LSM 510 Meta confocal microscope (Axiovert 200M), which was equipped with HeNe (633 nm), HeNe (543 nm), and Ar (488 nm) lasers. Three-dimensional, multichannel image-processing software (IMARIS, Bitplane AG, Zurich, Switzerland) was used to process the obtained microscopic images.

Transmission Electron Microscopy

Tumor samples were harvested and processed as described in Djonov et al.[33] They were stained with lead citrate and uranyl acetate before viewing in a Philips EM-400 transmission electron microscope.

5-Bromo-2′-Deoxyuridine Staining

Three hours before sacrifice the mice whose tumors were to be harvested for the paraffin sectioning were injected

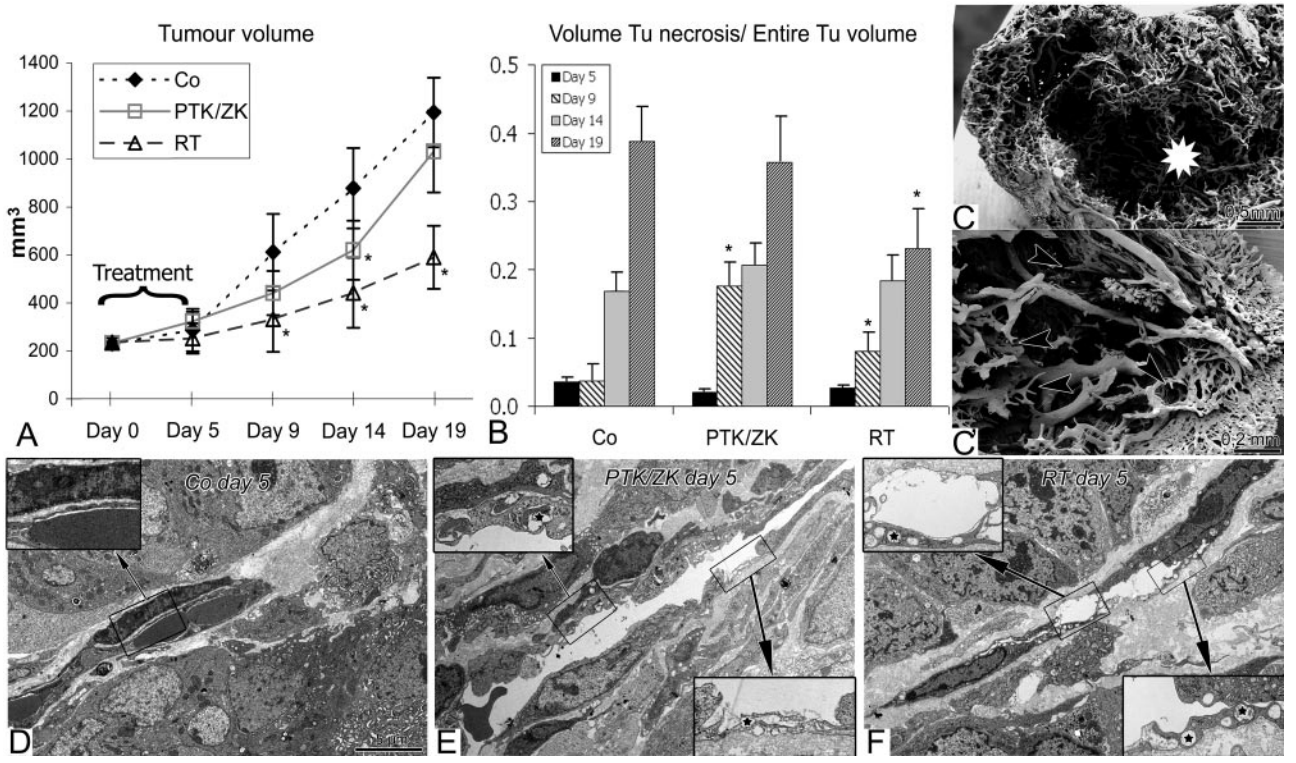

Figure 1. The graph (**A**) and bar graph (**B**) showing tumor growth delay and central necrosis. **A, B**: PTK/ZK and radiation delayed tumor growth (**A**) and induced central necrosis (estimated as a ratio "volume tumor necrosis/entire tumor volume") (**B**). Mean values ($n \geq 3$) are represented together with the SD. *Value is significantly different from the control ($^*P \leq 0.02$). Tumor growth was inhibited by both treatment strategies. **C, C′**: Vascular casts of MMTV/c-neu mammary carcinoma xenografts, on day 5 (**C**) and day 9 (**C′**) after onset of treatment with PTK/ZK. Large avascular areas (**asterisks**) are apparent within the medullary region. Multiple tiny capillary sprouts emanate from the preserved cortical vessels and invade the avascular medulla (**arrowheads**). **D–F**: Transmission electron micrographs illustrating changes in the vessels. In (**D**), a vessel in a non-treated tumor with intact endothelium is shown. **E, F**: Attenuation with partial denudation (see inserts) and vacuolization (**asterisks**) of endothelial cells in the tumor vessels after treatment with PTK/ZK (**E**) or irradiation (**F**). The magnification is ×3600; the scale bar is presented in (**D**).

intraperitoneally with 0.3 ml of a 20 mg/ml 5-bromo-2′-deoxyuridine (BrdU) solution. For BrdU staining, 3-μm-thick paraffin sections of the harvested tumors were processed according to Birner et al.[34] The primary antibody used: mouse anti-BrdU, diluted 1:100 (B-2531, Sigma, Buchs, Switzerland). Detection of anti-BrdU binding was performed using an avidin-peroxidase system (A-3151; Sigma, Buchs, Switzerland).

Hypoxia-Inducible Factor-1α Immunostaining

For hypoxia-inducible factor (HIF)-1α staining, 3-μm-thick paraffin sections of the harvested tumors were processed according to Gruber et al.[35] The primary antibody used was monoclonal antibody H1a67 (Novus Biologicals, Littleton, CO) diluted 1:5000 for 30 minutes at ambient temperature. The biotinyl tyramide amplification reagent was diluted 1:10 in protein blocking solution (Dako, Carpinteria, CA).

Results

PTK/ZK and Radiation Inhibit Tumor Growth and Induce Central Necrosis

Mice bearing xenografts derived from c-neu-overexpressing murine mammary adenocarcinoma cells were treated on 4 consecutive days with the VEGF-receptor tyrosine-kinase inhibitor PTK/ZK (4 × 100 mg/kg) or with ionizing radiation (4 × 3 Gy). To determine the time course of tumor growth- and treatment-dependent tumor necrosis the size of tumors were determined by caliper measurements and tumors from the different treatment groups were harvested on days 5, 9, 14, and 19 after the onset of treatment. The growth inhibitory effect was statistically significant ($P < 0.02$) for both treatment groups at day 14 and at days 9 and 19 for radiation treatment (Figure 1A). On days 9 and 14, central necrosis embraced a larger relative volume in both treatment groups than in the control animals (Figure 1B). In the both treatment groups, casts of the tumor vasculature revealed the medullary plexus to be completely destroyed. A large central avascular area was apparent, and this probably corresponded to the necrotic region (Figure 1C). The time courses of the changes were different after anti-angiogenic and radiotherapy (Figure 1B). In the mice that were treated with PTK/ZK or radiation, central necrosis on day 9 was significantly greater than in the control tumors. On day 19 there was no difference between tumors from PTK/ZK treated mice or control mice, whereas tumors from mice treated with radiation showed less central necrosis on day 19. After either treatment, cortical vessels and larger medullary vessels remained perfused on day 9 and had pillars and meshes, signs of ongoing intussus-

ception. Many tiny capillary sprouts emanated from the preserved cortical vessels and invaded the avascular medulla (Figure 1C′). At the ultrastructural level the attenuation with partial denudation and vacuolization of endothelial cells in the vasculature of treated tumors on day 5 (Figure 1, E and F) was evident. In the non-treated tumors the endothelium was intact (Figure 1D).

The Survival of Cortical Vessels Is Linked to the Presence of SMA-Positive Cells

One day after the cessation of treatment with PTK/ZK (day 5), the medullary capillary plexus was completely destroyed. The functionally preserved cortical region usually occupied a breadth of 0.5 to 1 mm (Figure 1, C–C′). In untreated tumors (Figure 2, A–C′), the tumor cortex was well supplied with small vessels that bore a covering of SMA-positive cells (Figure 2, B–B′). In contrast, microvessels located within the medulla were generally SMA-negative (Figure 2, C–C′). This spatial distribution revealed by immunohistochemistry corresponded to the pattern revealed by immunoblotting for SMA (Figure 2D) and reflected the stage of vascular maturation. Combined with the aforementioned preservation of mainly cortical or larger medullary vessels, these results indicate that the anti-angiogenic effects of radiotherapy or PTK/ZK were confined to the immature vessels, which were located in the medulla. The more mature cortical vessels with a peri-endothelial covering were resistant to both treatment modalities.

Revascularization and Recovery of the Tumor Stem from SMA-Positive Vessels in the Cortex

To determine whether revascularization and recovery of the tumor originates from SMA-positive vessels in the cortex, the proliferative capacity was determined in response to radiation therapy or PTK/ZK treatment using BrdU-immunostaining. From day 5 onwards, tumors underwent revascularization and recovery. On day 5, an obvious difference in the number of proliferating cells was observed between the cortex and the medulla in both treatment groups (Figure 3, A–B). The proliferating cells were detected mainly in periphery of the tumor. Thereafter the overall proliferative rate of tumor cells increased and the difference between cortex and medulla diminished (Figure 3C). Quantification of the number of proliferating tumor cells within the cortical and the medullary regions disclosed a rapid recovery in the PTK/ZK-treated group and a slower one in the animals that had undergone radiotherapy, indicative for a stronger antiproliferative effect of radiation than for PTK/ZK (Figure 3B). Proliferative activity correlated positively with tumor volume and negatively with the relative volume of central necrosis (Figure 1, A–B).

Tumor Recovery Is Associated with Intussusceptive Microvascular Growth

Besides formation of capillary sprouts originating from the cortical plexus, first augmentations of intussusceptive angiogenesis were observed immediately after cessation of therapy in the PTK/ZK-treated tumors. Between day 9 and 14, the vasculature in both treated groups expanded predominantly by intussusception: the intratumoral plexus consisted of large sinusoidal vessels and casts of the vessels revealed the presence of numerous tiny holes, the hallmarks of intussusceptive angiogenesis (Figure 4, D, F). These holes represented transluminal tissue pillars, which were digested during the process of maceration. Quantification of the number of newly formed pillars (with a diameter of less than 2.5 μm) per vascular area on day 9 revealed a significant increase in both treatment groups (Figure 4G). By day 19, intussusception had given way to a second wave of sprouting angiogenesis (Figure 4H). At this latter juncture, the ratio of sprouts to pillars in the PTK/ZK-treated group was similar to that in the control mice. In the tumors that had undergone radiotherapy, the sprout numerical density was significantly higher, indicating an even more pronounced stress response.

The Specific Time-Course of the Changes in the Vascular Pattern of Treated Tumors

The vascular pattern of the non-treated tumors was characterized mainly by sprouting mode of angiogenesis (see Figure 4B). As shown in Figure 5A, the vascular pattern of the treated tumors had its specific time-course: the signs of intussusception were prevalent on day 6 (Figure 5A) and day 14 (Figure 5A′). Noteworthy, that on day 6 there were not only pillars, but also meshes apparent (Figure 5A). The appearance of the meshes needs a relatively longer time; therefore the intussusception had been activated already by the end of the treatment if not during it. On day 19 the vascular pattern was characterized by numerous sprouts (arrows in Figure 5A′′) with still present but fewer signs of intussusception indicating the second wave of sprouting.

The scheme in Figure 5B presents the time-course specific changes in the angiogenesis mode (switch sprouting to intussusception) after the therapy cessation in comparison with non-treated tumors.

Tumor Recovery Is Associated with a Dramatic Decrease in Intratumoral Microvascular Density, but with Only a Non-Significant One in the Vascular Exchange Surface

Intratumoral microvascular density (IMD) is widely used as a gauge of tumor behavior. A high IMD, being equated with high metabolic activity, is presumed to forebode an unfavorable prognosis and outcome. Vessel area density (VAD), also defined as total microvascular area,[36] is a parameter representing more directly the blood supply and in this way probably better correlates with the transendothelial transport of nutrients and oxygen, and thus with the vasculature-related metastatic potential of the neoplasm.

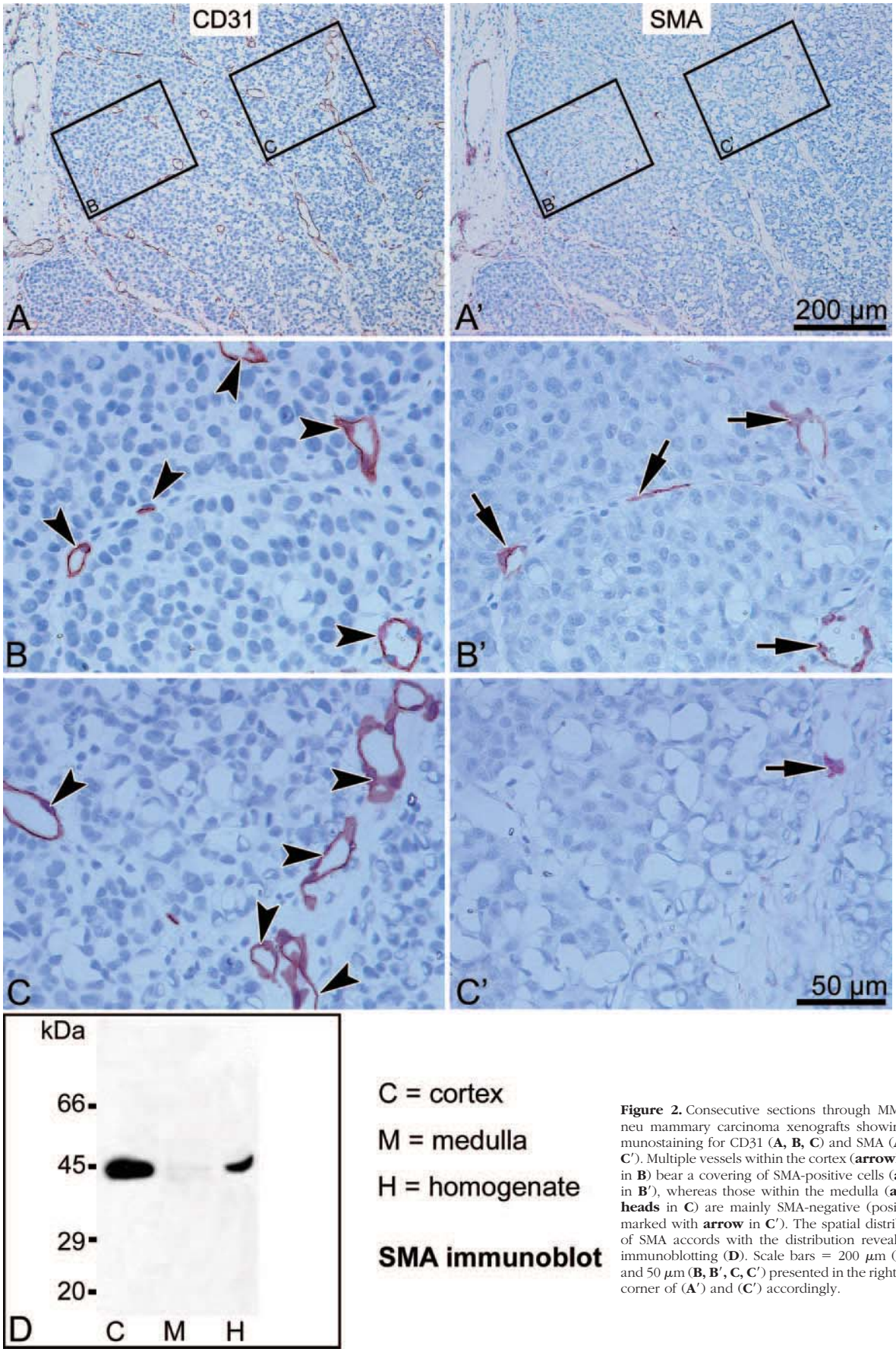

Figure 2. Consecutive sections through MMTV/c-neu mammary carcinoma xenografts showing immunostaining for CD31 (**A, B, C**) and SMA (**A′, B′, C′**). Multiple vessels within the cortex (**arrowheads** in **B**) bear a covering of SMA-positive cells (**arrow** in **B′**), whereas those within the medulla (**arrowheads** in **C**) are mainly SMA-negative (positive is marked with **arrow** in **C′**). The spatial distribution of SMA accords with the distribution revealed by immunoblotting (**D**). Scale bars = 200 μm (**A, A′**) and 50 μm (**B, B′, C, C′**) presented in the right lower corner of (**A′**) and (**C′**) accordingly.

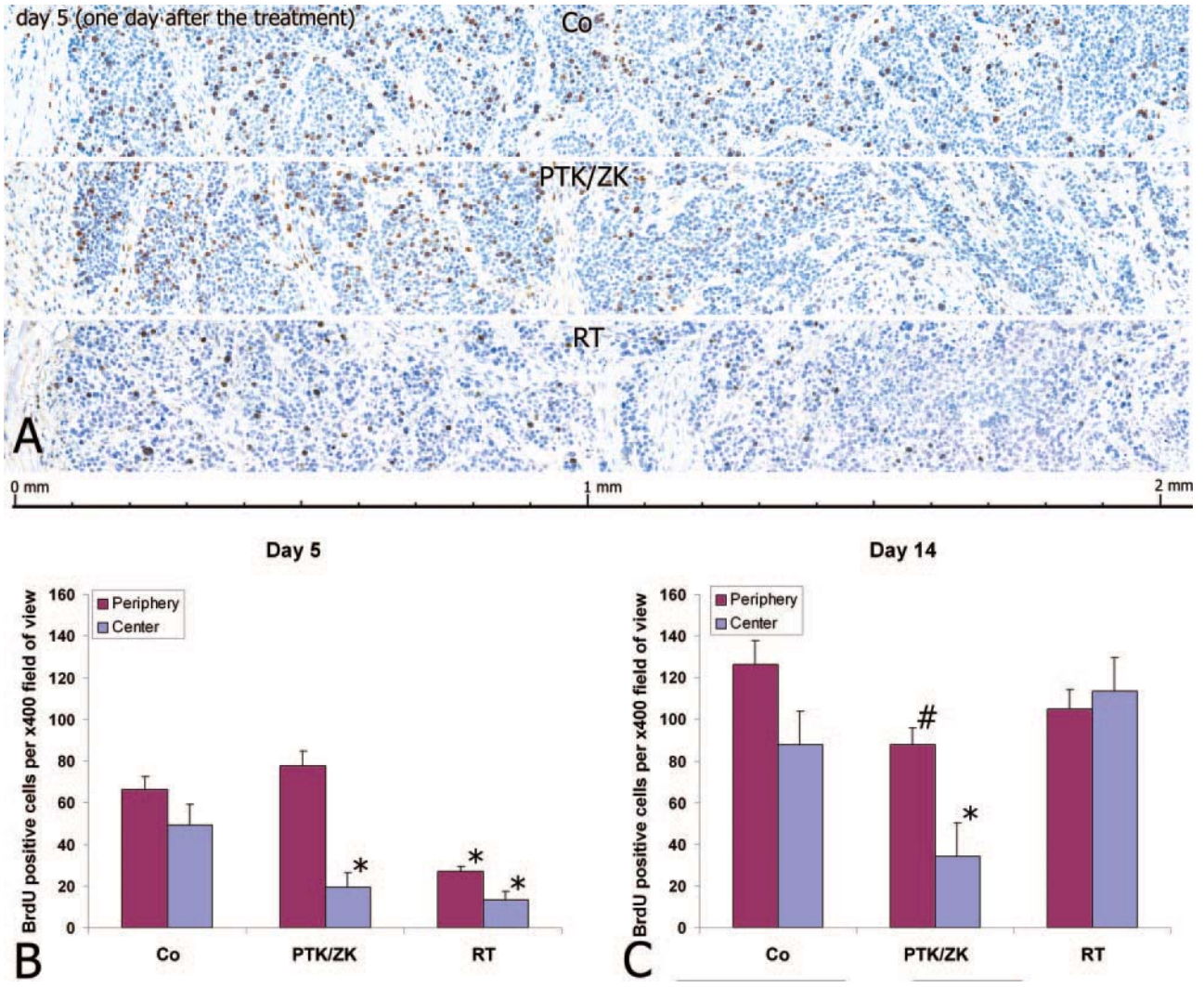

Figure 3. Proliferative activity of tumor cells on day 5 visualized by BrdU immunostaining revealed treatment-specific spatial tumor recovery (**A**). The outer "ring" of the tumor with the breadth of up to 1 mm was characterized by the maximal proliferating activity. The counting of BrdU-positive cells on days 5 and 14 indicated a specific time-course of tumor recovery (**B**). On day 14 the overall proliferative rate of tumor cells increased and the difference between cortex and medulla diminished (**C**). The values significantly different from control values are marked with $^{*}(P \leq 0.02)$ or $^{\#}(P \leq 0.05)$.

The CD31-immunostaining revealed qualitative differences in the vascular pattern of different groups (Figure 6A–C). The subsequent quantification demonstrated the decrease of the IMD in both treated and of the VAD in the irradiated group on day 5 (Figure 6D). On day 9 the IMD was still decreased by more than 40% in the PTK/ZK-treated group and by more than 30% in the irradiated tumors. In contrast, the VAD was only slightly lower at this juncture (Figure 6E). By day 19, the IMD was increased in each of the treated groups, whereas the VAD remained unchanged (Figure 6F). The differential effect on IMD and VAD mirrors the onset of the treatment-induced intussusception; intussusceptive angiogenesis leads to the stretching of the endothelium and formation of large, sinusoidal vessels. This phenomenon counterbalanced the decrease of the IMD, thus enabling the tumor vasculature to maintain its functional capacity (ie, without compromising the VAD).

The HIF-1α staining of the tumor samples harvested on day 14 has corroborated the finding that the functional capacity of the vasculature was adequately maintained (Figure 6, G–I). In the control tumor there were HIF-1α-positive cells at in the typical arrangement surrounding the microvessels (Figure 6G); in both treated groups there was no such pattern revealed the tumor cells were mainly HIF-1α-negative (Figure 6, G–I). The blood supply to the tumor cells in treated groups appeared to be yet improved in the recovery period if compared with the control group.

Tumor Recovery Is Associated with Up-Regulation of SMA

One of the crucial steps of intussusception is invasion of interstitial pillar cores with pericytes, SMA-positive cells and myofibroblasts, which lay down collagen fibrils. By this stage, the transluminal pillars have a diameter of less than 2.5 μm. In the subsequent phase, the pillars increase in girth by additional recruitment of peri-endothe-

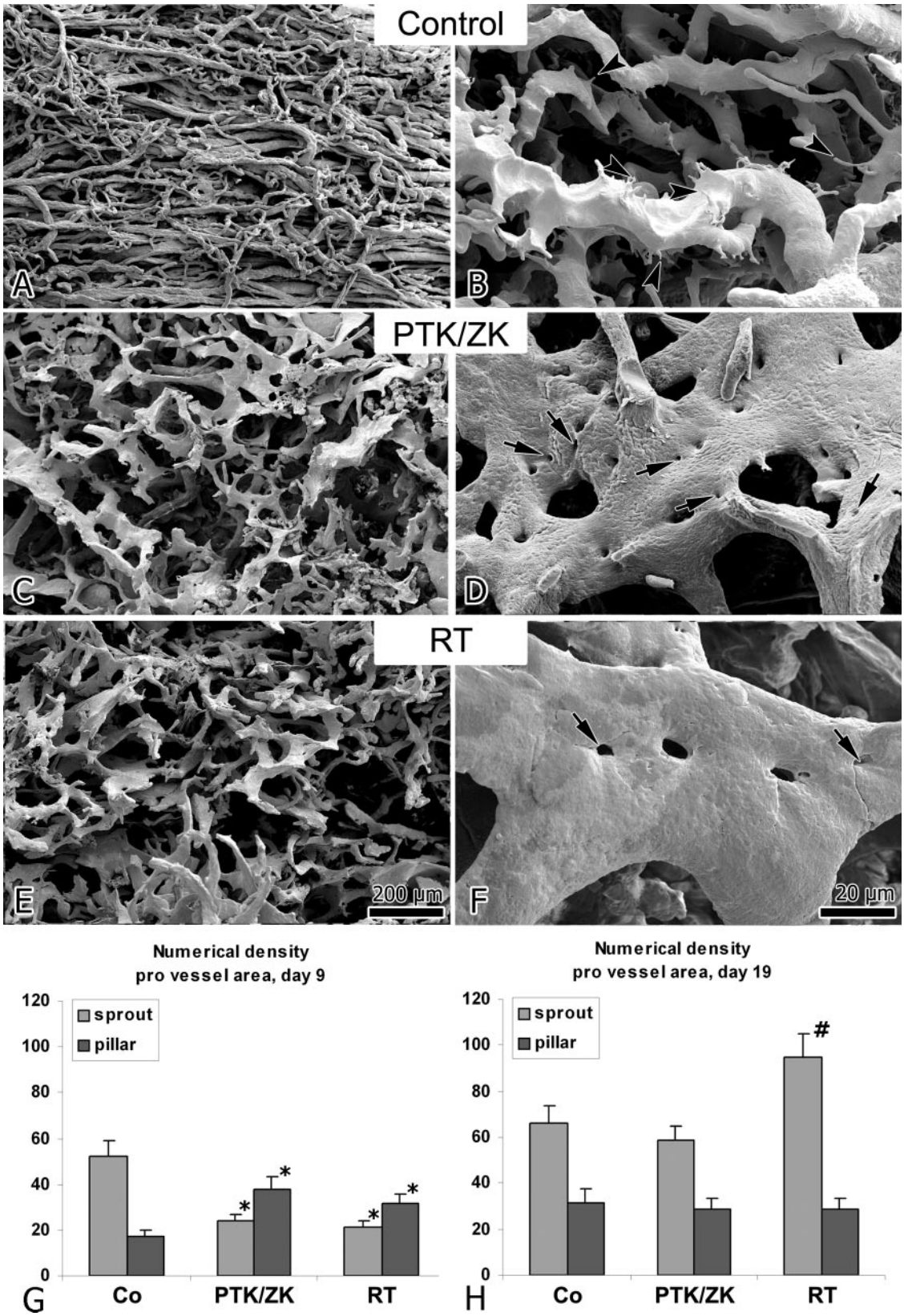

Figure 4. A–F: Vascular casts of MMTV/c-neu mammary carcinoma xenografts on day 14 revealing a change in the mode of vascular growth from sprouting (in control animals) to intussusception (after treatment with PTK/ZK or irradiation). The revascularization process involves mainly intussusceptive angiogenesis, as evidenced by the presence of numerous tiny holes in the casts (**arrows**). In the control tumors, vascular growth occurs predominantly by sprouting (**arrowheads**). **G, H**: Bar graphs showing the number of newly-formed pillars (with a diameter of less than 2.5 μm) and sprouts per vascular surface on days 9 (**G**) and 19 (**H**). The values significantly different from control values are marked with $^{*}(P \leq 0.02)$ or $^{\#}(P \leq 0.05)$.

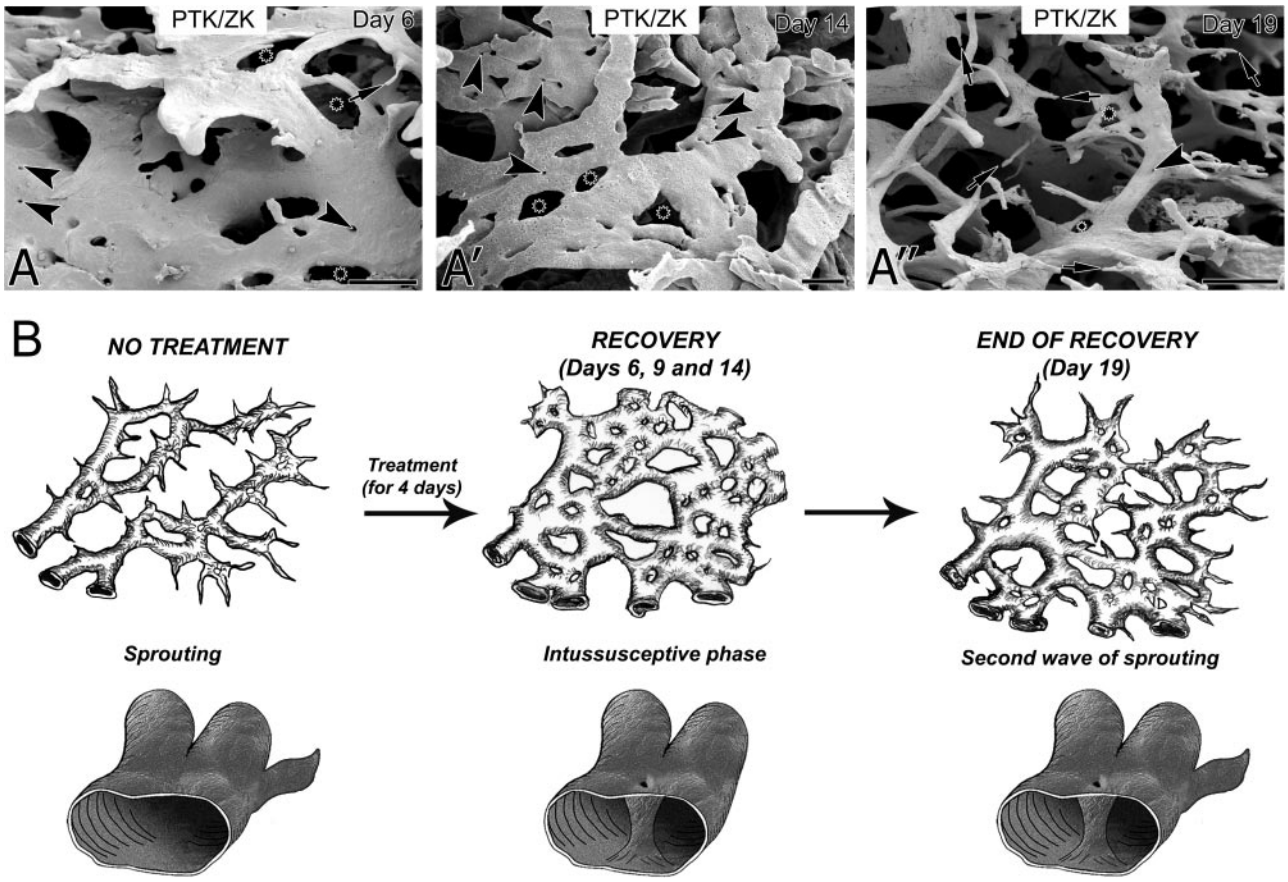

Figure 5. Micrographs and schema illustrating time-course of the angiogenic switch during tumor recovery. The scanning electron micrographs representing the vascular pattern of the PTK/ZK treated tumors on day 6 (**A**), 14 (**A′**), and 19 (**A″**). On day 6 and 14 pillars (**arrowheads**) and meshes (**asterisks**) dominate. In contrast to days 6 and 14, on day 19 (**A″**) the sprouts (**arrows**) prevail in the vascular pattern of the PTK/ZK-treated tumors with some pillars (**arrowhead**) or meshes (**asterisks**) present. The bar in (**A–A″**) is 100 μm. The scheme in **B** represents the above-described changes: in non-treated tumors the dominating mode of angiogenesis is sprouting. After the short-term therapy the intussusception prevails: so called, intussusceptive phase of recovery (days 6, 9, and 14). On day 19 the second wave of intussusception is there what is characterized by numerous sprouts along with pillars or meshes.

lial cells and deposition of extracellular matrix proteins, without undergoing any further change in their structure. The so-formed large pillars (termed also meshes) are robust structures that are unlikely to regress.

The light and laser scanning confocal microscopy revealed numerous SMA-positive cells to be located not only in the vicinity of the pillars (Figure 7, A), but also as a robust multilayered peri-endothelial covering (Figure 7, B–B′′′). SMA-immunoblotting disclosed higher levels in the medulla than in the cortical region of tumors on day 9 (Figure 7C). This finding indicates that during the process of tumor recovery adaptive changes were triggered in the medullary vessels.

Discussion

The recovery of tumors after therapy is a major problem in the management of cancer patients. The regrowth of neoplasms after cytotoxic treatment is attributable to the proliferation of a subpopulation of treatment resistant, often hypoxic tumor cells.[37] Tumor angiogenesis is generally deemed to be crucial for the growth and dissemination of tumors, which is the rationale for the application of angiogenesis inhibitors as cancer therapy. A broad spectrum of such agents (mainly VEGF inhibitors) have been tested on the preclinical and clinical level.[6,7,14] Even though angiogenesis inhibitors induce a partial regression of tumor vessels and elicit a reduction in tumor size, the effects are transient and long-term results are disappointing.[15,38–40] During tumor recovery remodeling of blood vessels in conjunction with the proliferation of tumor cells might be part of adaptive mechanisms that allow recovery of the tumor and contribute to the development of resistance to therapy.

In our report we suggest that a window of intussusception after angiogenesis inhibition occurs as an adaptive mechanism to restore and maintain vascular function after treatment related damage. The detailed analysis of the morphological changes demonstrates a switch from sprouting to intussusceptive angiogenesis, which occurs not only after treatment cessation with this inhibitor of angiogenesis but also during the recovery period from fractionated irradiation. After exposure to PTK/ZK or ionizing radiation, the sinusoidal-like vessels were characterized by numerous transluminal tissue pillars. These pillars are hallmarks of intussusceptive angiogenesis. Of note, intussusceptive angiogenesis after treatment with PTK/ZK has already been documented (albeit unbe-

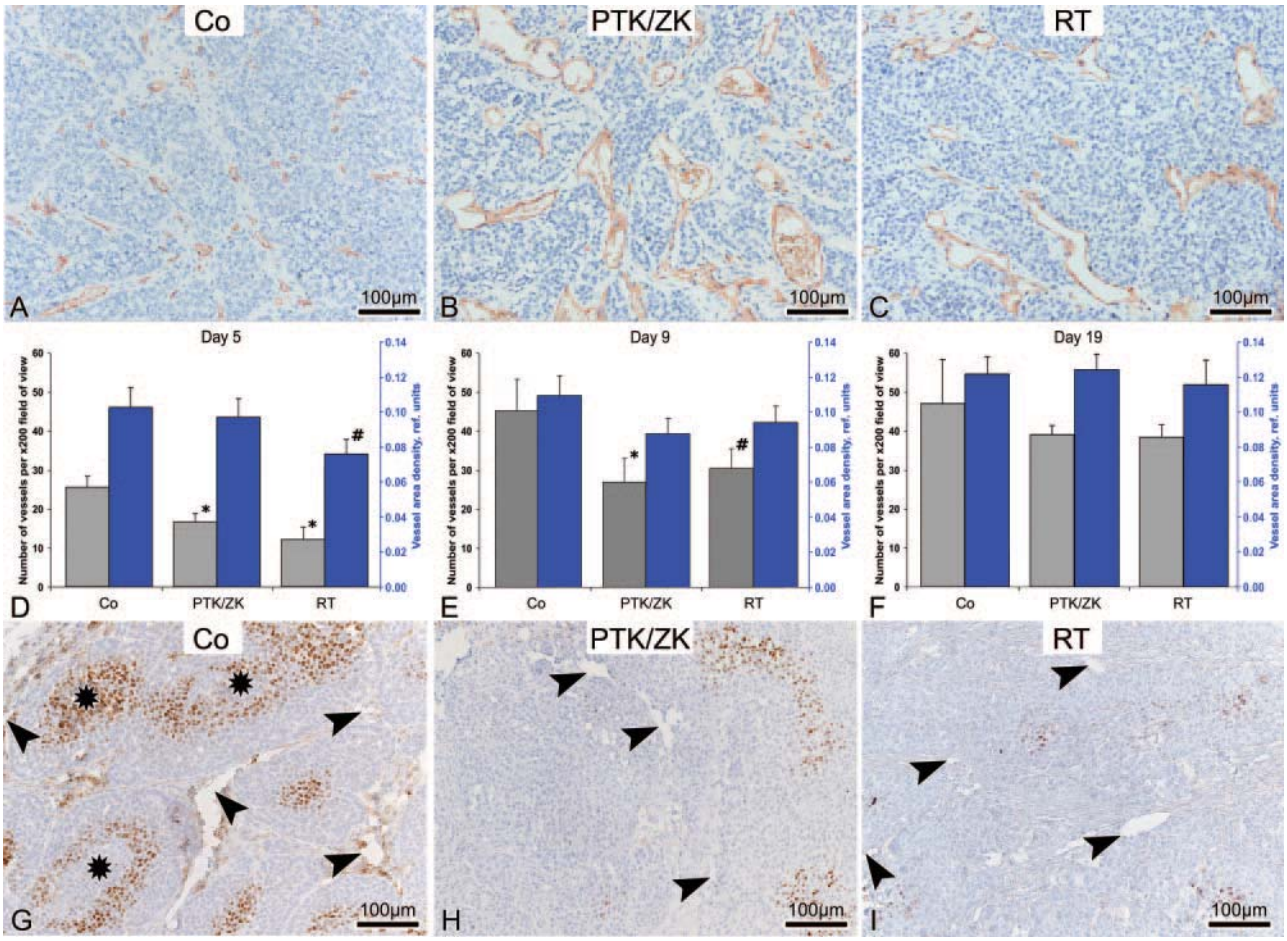

Figure 6. A–C: Immunohistochemical staining of MMTV/c-neu mammary carcinoma xenografts for CD31 revealing a multitude of tiny vessels in control tumors and fewer, but larger sinusoidal ones in the treated groups. **D–F**: Changes in the IMD; number of vessels per ×200 field of view) and vessel area density on days 5, 9, and 19 reflect a switch in the mode of angiogenesis: intussusception on day 9 and a second wave of sprouting on day 19. The values significantly different from control values are marked with *($P \leq 0.02$) or #($P \leq 0.05$). The HIF-1α staining (**G–I**) reveals the differences in oxygenation level of the tumor cells on day 14: in non-treated tumors (**G**) there is apparent hypoxia demonstrated by plentiful HIF-1α-positive cells on the distance of more than 100 to 130 μm from the vessels (**arrowheads** in **G–I**). There are necrotic areas on similar distances from the vessels (**asterisks** in G). On day 14 in both treated groups the level of oxygenation is apparently better with only some HIF-1α-positive cells (**H** and **I**). The vessels are marked with **arrowheads** (**G–I**). The magnification is ×200.

known to the authors) in other tumor models, such as in a murine renal cell carcinoma study including treatment with PTK/ZK.[19] In this study PTK/ZK elicited changes in the vasculature that are typical of intussusception, namely, the appearance of large sinusoidal-like vessels and an increase in the intervascular distance. On the other hand the vessel density decreased by as much as 48%, and the systolic blood-flow velocity in the renal artery remained unchanged. The relative tumor blood volume increased by 44%, and the vessel permeability decreased by 50%.[19] Furthermore, although the demonstrated vascular casts clearly revealed the presence of transluminal pillars, the authors did not recognize the phenomenon of intussusceptive angiogenesis. Similar morphological and hemodynamic changes in the vasculature have been observed in murine orthotopic B16/BL6 melanoma tumor model after treatment with either PTK/ZK[41] or other tyrosine kinase inhibitors, such as KRN951,[42] CEP-7055,[43] and KRN633.[44] In each instance, the described changes in the vessels correspond to those associated with intussusceptive angiogenesis. Intussusceptive angiogenesis might represent a general process as part of a tumor-protective adaptive response.

A switch from sprouting to intussusceptive angiogenesis might represent an adaptive response to treatment with various anti-tumor and anti-angiogenic compounds. Exposure of rat hepatic carcinomas to sirolimus (an mTOR-kinase inhibitor with anti-proliferative and anti-angiogenic properties) impaired tube formation and the vascular sprouting of aortic rings *in vitro*.[25] Furthermore, the surviving vessels in SK-NEP-1 tumor xenografts in mice after treatment with VEGF-Trap, were sinusoidal-like and centrally located in the viable and growing tumor regions. These vessels bore a coverage of SMA-positive peri-endothelial cells.[45] Likewise, tumor recovery after treatment with AG-013736 or AG-028262 (inhibitors of VEGF-receptor signaling) in the RIP-Tag 2 and Lewis lung carcinoma models was associated not only with rapid revascularization with the denuded sleeves of basement membrane serving as a scaffold: the high-quality images also demonstrated definite evidence of intussusceptive angiogenesis.[46]

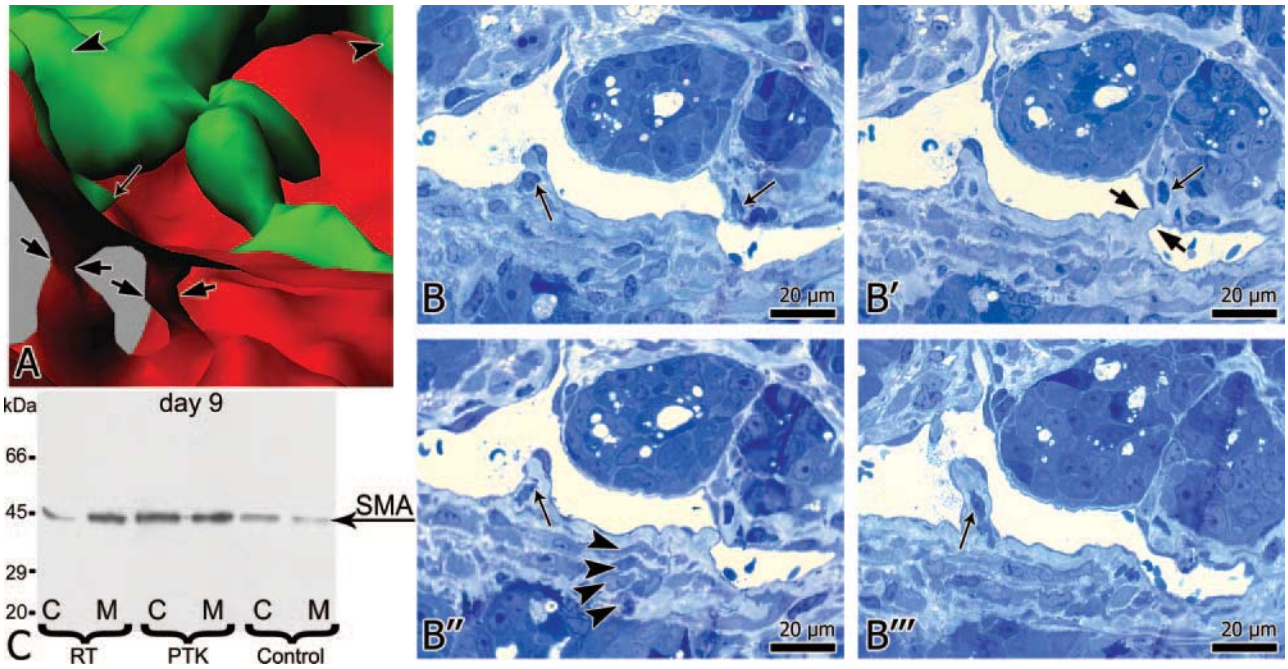

Figure 7. Spatial distribution of SMA on day 9. **A, B**: Laser scanning microscopy (**A**) of double-immunostaining [CD31-red (endothelium); SMA-green (SMA-positive cells)] and light microscopic inspection of toluidine-blue-stained consecutive sections (**B–B‴**) revealed that SMA-positive cells are located in the vicinity of pillars (**arrows** in **A** and **B**) and also as peri-endothelial covering (**arrowheads** in **A** and **B**). The double **arrows** in **A** and **B** indicate transluminar tissue pillars. **C**: Estimation of SMA by immunoblotting revealed higher levels in the medullary than in the cortical tumor regions. (C = cortex, M = medulla).

In primary human tumors, as well as in murine tumor models, inhibition of VEGF/VEGFR signaling induces selective apoptosis of endothelial cells in immature capillaries. In contrast, mature vessels with a coverage of peri-endothelial cells survive VEGF withdrawal.[47] In a recent publication, treatment with PTK/ZK in the B16/BL6 melanoma tumor model induced a significant decrease in vessel density within cervical metastases but not within primary tumors.[41] These findings most probably reflect the relative immaturity of the vascular plexus in metastases compared to the vasculature in the primary tumor. Our own recent data on nonmalignant vessels in the developing chorioallantoic membrane of the chicken also demonstrated that exposure to PTK/ZK induced significant regression of the vasculature on embryonic day 8, but had no effect on day 12, a stage at which microvessels are already covered with pericytes.[48]

In the present study transmission electron microscopy data revealed that exposure of the tumors to PTK/ZK or ionizing radiation led to attenuation with partial denudation and vacuolization of endothelial cells in the tumor vessels and subsequent instability of the vessel walls. In another ongoing study we have observed by epifluorescence microscopy after injection of fluorescein isothiocyanate-dextran solution that irradiation induces focally increased permeability of vessels. Electron microscopy has revealed that the irradiated vasculature has the same morphological alterations as presented here for the tumor vessels of both treatment groups. These findings suggest that the morphological changes after irradiation are ubiquitous. The described changes in the vasculature and its altered permeability explain the frequent occurrence of extravasates in the vascular casts of tumors immediately after the treatment cessation (day 5, data not shown), which prevented quantification of the casts at this time point. In contrast, the occurrence of extravasates had no crucial influence on the quality of the vascular casts made on days 9, 14, and 19. Such time-course indicates that by day 9 the tumoral vascular tree had undergone substantial remodeling, presumably by vascular pruning. The signs of intussusception are already seen on day 6, as demonstrated in Figure 5A′. Therefore, the angiogenic switch to intussusception probably takes place already during the therapy or immediately after its cessation. Moreover, we observed that exposure to PTK/ZK or ionizing radiation destroyed mainly the immature medullary vascular plexus while cortical vessels, which bear a coverage of SMA-positive cells, remained perfused. Tumor recovery originated from the morphologically and functionally preserved cortical region with the number of proliferating tumor cells decreasing progressively from the cortical to the medullary region, in accord with a decrease in the density of the vessels.

Following cessation of treatment, the inhibitory effects of PTK/ZK and ionizing radiation on tumor growth abated after about one week. Tumor regrowth coincides with the second wave of sprouting angiogenesis. A transient switch from sprouting to intussusceptive angiogenesis may be an adaptive response to restore the hemodynamic and structural properties of the vasculature (see scheme in Figure 5B). Intussusceptive remodeling and probably pruning accompanied by the recruitment of SMA-positive cells restores the tumor vasculature. This is characterized by a low rate of endothelial proliferation and by low transendothelial permeability. In this study the HIF-1α-staining clearly represents the sufficient oxygen

supply to the tumor cells 10 days after the treatment cessation. Moreover, using high resolution small animal positron emission tomography in a mouse mammary cancer allograft model, we recently demonstrated that the same schedule of PTK/ZK treatment resulted in enhanced tumor hypoxia by the end of treatment, but reoxygenation was again prevalent by day 14 (10 days after treatment cessation).[49] The angiogenic switch from sprouting to intussusception in response to inhibition of angiogenesis represents a part of angio-adaptive mechanism that most probably serves to repair a damaged tumor vasculature to restore the oxygen supply to the tumor.

Overall, our data indicate that an angiogenic switch from sprouting to intussusceptive angiogenesis occurs after treatment with the angiogenesis inhibitor or radiation and may be part of a tumor-protective adaptive response. In addition, the radiation-induced vascular damage observed supports the concept that tumor vasculature is one of the prime targets for radiation.

Acknowledgments

We thank Krystyna Sala, Bettina de Breuyn, Barbara Krieger and Regula Buergy for their excellent technical support. Dr. Andrew Makanya is kindly acknowledged for the critical reading of the manuscript.

References

1. Winkler F, Kozin SV, Tong RT, Chae SS, Booth MF, Garkavtsev I, Xu L, Hicklin DJ, Fukumura D, di Tomaso E, Munn LL, Jain RK: Kinetics of vascular normalization by VEGFR2 blockade governs brain tumor response to radiation: role of oxygenation, angiopoietin-1, and matrix metalloproteinases. Cancer Cell 2004, 6:553–563
2. Ferrara N, Kerbel RS: Angiogenesis as a therapeutic target. Nature 2005, 438:967–974
3. Jain RK: Normalization of tumor vasculature: an emerging concept in antiangiogenic therapy. Science 2005, 307:58–62
4. Kerbel RS: Antiangiogenic therapy: a universal chemosensitization strategy for cancer? Science 2006, 312:1171–1175
5. Marx J: Angiogenesis. A boost for tumor starvation. Science 2003, 301:452–454
6. Duda DG: Antiangiogenesis and drug delivery to tumors: bench to bedside and back. Cancer Res 2006, 66:3967–3970
7. Sivakumar B, Harry LE, Paleolog EM: Modulating angiogenesis: more vs less. JAMA 2004, 292:972–977
8. Ferrara N, Gerber HP, LeCouter J: The biology of VEGF and its receptors. Nat Med 2003, 9:669–676
9. Ferrara N: Vascular endothelial growth factor: basic science and clinical progress. Endocr Rev 2004, 25:581–611
10. Kramer I, Lipp HP: Bevacizumab, a humanized anti-angiogenic monoclonal antibody for the treatment of colorectal cancer. J Clin Pharm Ther 2007, 32:1–14
11. Hurwitz H, Kabbinavar F: Bevacizumab combined with standard fluoropyrimidine-based chemotherapy regimens to treat colorectal cancer. Oncology 2005, 69 Suppl 3:17–24
12. Gerber HP, Ferrara N: Pharmacology and pharmacodynamics of bevacizumab as monotherapy or in combination with cytotoxic therapy in preclinical studies. Cancer Res 2005, 65:671–680
13. Force T, Kuida K, Namchuk M, Parang K, Kyriakis JM: Inhibitors of protein kinase signaling pathways: emerging therapies for cardiovascular disease. Circulation 2004, 109:1196–1205
14. Eskens FA: Angiogenesis inhibitors in clinical development; where are we now and where are we going? Br J Cancer 2004, 90:1–7
15. Bergers G, Song S, Meyer-Morse N, Bergsland E, Hanahan D: Benefits of targeting both pericytes and endothelial cells in the tumor vasculature with kinase inhibitors. J Clin Invest 2003, 111:1287–1295
16. Erber R, Thurnher A, Katsen AD, Groth G, Kerger H, Hammes HP, Menger MD, Ullrich A, Vajkoczy P: Combined inhibition of VEGF and PDGF signaling enforces tumor vessel regression by interfering with pericyte-mediated endothelial cell survival mechanisms. FASEB J 2004, 18:338–340
17. Thomas AL, Morgan B, Drevs J, Unger C, Wiedenmann B, Vanhoefer U, Laurent D, Dugan M, Steward WP: Vascular endothelial growth factor receptor tyrosine kinase inhibitors: pTK787/ZK 222584. Semin Oncol 2003, 30:32–38
18. Wood JM, Bold G, Buchdunger E, Cozens R, Ferrari S, Frei J, Hofmann F, Mestan J, Mett H, O'Reilly T, Persohn E, Rosel J, Schnell C, Stover D, Theuer A, Towbin H, Wenger F, Woods-Cook K, Menrad A, Siemeister G, Schirner M, Thierauch KH, Schneider MR, Drevs J, Martiny-Baron G, Totzke F: PTK787/ZK 222584, a novel and potent inhibitor of vascular endothelial growth factor receptor tyrosine kinases, impairs vascular endothelial growth factor-induced responses and tumor growth after oral administration. Cancer Res 2000, 60:2178–2189
19. Drevs J, Muller-Driver R, Wittig C, Fuxius S, Esser N, Hugenschmidt H, Konerding MA, Allegrini PR, Wood J, Hennig J, Unger C, Marme D: PTK787/ZK 222584, a specific vascular endothelial growth factor-receptor tyrosine kinase inhibitor, affects the anatomy of the tumor vascular bed and the functional vascular properties as detected by dynamic enhanced magnetic resonance imaging. Cancer Res 2002, 62:4015–4022
20. Garcia-Barros M, Paris F, Cordon-Cardo C, Lyden D, Rafii S, Haimovitz-Friedman A, Fuks Z, Kolesnick R: Tumor response to radiotherapy regulated by endothelial cell apoptosis. Science 2003, 300:1155–1159
21. Paris F, Fuks Z, Kang A, Capodieci P, Juan G, Ehleiter D, Haimovitz-Friedman A, Cordon-Cardo C, Kolesnick R: Endothelial apoptosis as the primary lesion initiating intestinal radiation damage in mice. Science 2001, 293:293–297
22. Koukourakis MI, Giatromanolaki A, Sivridis E, Simopoulos K, Pissakas G, Gatter KC, Harris AL: Squamous cell head and neck cancer: evidence of angiogenic regeneration during radiotherapy. Anticancer Res 2001, 21:4301–4309
23. Lovey J, Lukits J, Remenar E, Koronczay K, Kasler M, Nemeth G, Timar J: Antiangiogenic effects of radiotherapy but not initial microvessel density predict survival in inoperable oropharyngeal squamous cell carcinoma. Strahlenther Onkol 2006, 182:149–156
24. Hess C, Vuong V, Hegyi I, Riesterer O, Wood J, Fabbro D, Glanzmann C, Bodis S, Pruschy M: Effect of VEGF receptor inhibitor PTK787/ZK222584 [correction of ZK222548] combined with ionizing radiation on endothelial cells and tumour growth. Br J Cancer 2001, 85:2010–2016
25. Semela D, Piguet AC, Kolev M, Schmitter K, Hlushchuk R, Djonov V, Stoupis C, Dufour JF: Vascular remodeling and antitumoral effects of mTOR inhibition in a rat model of hepatocellular carcinoma. J Hepatol 2007, 46:840–848
26. Burri PH, Hlushchuk R, Djonov V: Intussusceptive angiogenesis: its emergence, its characteristics, and its significance. Dev Dyn 2004, 231:474–488
27. Djonov V, Baum O, Burri PH: Vascular remodeling by intussusceptive angiogenesis. Cell Tissue Res 2003, 314:107–117
28. Gong QY, Eldridge PR, Brodbelt AR, Garcia-Finana M, Zaman A, Jones B, Roberts N: Quantification of tumour response to radiotherapy. Br J Radiol 2004, 77:405–413
29. United Kingdom Coordinating Committee on Cancer Res (UKCCCR) Guidelines for the Welfare of Animals in Experimental Neoplasia (Second Edition). Br J Cancer 1998, 77:1–10
30. Djonov VG, Kurz H, Burri PH: Optimality in the developing vascular system: branching remodeling by means of intussusception as an efficient adaptation mechanism. Dev Dyn 2002, 224:391–402
31. Ochs M, Fehrenbach H, Richter J: Ultrastructure of canine type II pneumocytes during hypothermic ischemia of the lung: a study by means of conventional and energy filtering transmission electron microscopy and stereology. Anat Rec 2001, 263:118–126
32. Makanya AN, Hlushchuk R, Baum O, Velinov N, Ochs M, Djonov V: Microvascular endowment in the developing chicken embryo lung. Am J Physiol Lung Cell Mol Physiol 2007, 292:L1136–L1146
33. Djonov V, Schmid M, Tschanz SA, Burri PH: Intussusceptive angiogenesis: its role in embryonic vascular network formation. Circ Res 2000, 86:286–292

34. Birner P, Ritzi M, Musahl C, Knippers R, Gerdes J, Voigtlander T, Budka H, Hainfellner JA: Immunohistochemical detection of cell growth fraction in formalin-fixed and paraffin-embedded murine tissue. Am J Pathol 2001, 158:1991–1996
35. Gruber G, Greiner RH, Hlushchuk R, Aebersold DM, Altermatt HJ, Berclaz G, Djonov V: Hypoxia-inducible factor 1 alpha in high-risk breast cancer: an independent prognostic parameter? Breast Cancer Res 2004, 6:R191–R198
36. Sharma S, Sharma MC, Sarkar C: Morphology of angiogenesis in human cancer: a conceptual overview, histoprognostic perspective and significance of neoangiogenesis. Histopathology 2005, 46: 481–489
37. Kim JJ, Tannock IF: Repopulation of cancer cells during therapy: an important cause of treatment failure. Nat Rev Cancer 2005, 5: 516–525
38. Ellis LM: Antiangiogenic therapy: more promise and, yet again, more questions. J Clin Oncol 2003, 21:3897–3899
39. Willett CG, Boucher Y, di Tomaso E, Duda DG, Munn LL, Tong RT, Chung DC, Sahani DV, Kalva SP, Kozin SV, Mino M, Cohen KS, Scadden DT, Hartford AC, Fischman AJ, Clark JW, Ryan DP, Zhu AX, Blaszkowsky LS, Chen HX, Shellito PC, Lauwers GY, Jain RK: Direct evidence that the VEGF-specific antibody bevacizumab has antivascular effects in human rectal cancer. Nat Med 2004, 10:145–147
40. Mayer RJ: Two steps forward in the treatment of colorectal cancer. N Engl J Med 2004, 350:2406–2408
41. Rudin M, McSheehy PM, Allegrini PR, Rausch M, Baumann D, Becquet M, Brecht K, Brueggen J, Ferretti S, Schaeffer F, Schnell C, Wood J: PTK787/ZK222584, a tyrosine kinase inhibitor of vascular endothelial growth factor receptor, reduces uptake of the contrast agent GdDOTA by murine orthotopic B16/BL6 melanoma tumours and inhibits their growth in vivo. NMR Biomed 2005, 18:308–321
42. Nakamura K, Taguchi E, Miura T, Yamamoto A, Takahashi K, Bichat F, Guilbaud N, Hasegawa K, Kubo K, Fujiwara Y, Suzuki R, Kubo K, Shibuya M, Isae T: KRN951, a highly potent inhibitor of vascular endothelial growth factor receptor tyrosine kinases, has antitumor activities and affects functional vascular properties. Cancer Res 2006, 66:9134–9142
43. Ruggeri B, Singh J, Gingrich D, Angeles T, Albom M, Yang S, Chang H, Robinson C, Hunter K, Dobrzanski P, Jones-Bolin S, Pritchard S, Aimone L, Klein-Szanto A, Herbert JM, Bono F, Schaeffer P, Casellas P, Bourie B, Pili R, Isaacs J, Ator M, Hudkins R, Vaught J, Mallamo J, Dionne C: CEP-7055: a novel, orally active pan inhibitor of vascular endothelial growth factor receptor tyrosine kinases with potent antiangiogenic activity and antitumor efficacy in preclinical models. Cancer Res 2003, 63:5978–5991
44. Nakamura K, Yamamoto A, Kamishohara M, Takahashi K, Taguchi E, Miura T, Kubo K, Shibuya M, Isoe T: KRN633: a selective inhibitor of vascular endothelial growth factor receptor-2 tyrosine kinase that suppresses tumor angiogenesis and growth. Mol Cancer Ther 2004, 3:1639–1649
45. Huang J, Frischer JS, Serur A, Kadenhe A, Yokoi A, McCrudden KW, New T, O'Toole K, Zabski S, Rudge JS, Holash J, Yancopoulos GD, Yamashiro DJ, Kandel JJ: Regression of established tumors and metastases by potent vascular endothelial growth factor blockade. Proc Natl Acad Sci USA 2003, 100:7785–7790
46. Mancuso MR, Davis R, Norberg SM, O'Brien S, Sennino B, Nakahara T, Yao VJ, Inai T, Brooks P, Freimark B, Shalinsky DR, Hu-Lowe DD, McDonald DM: Rapid vascular regrowth in tumors after reversal of VEGF inhibition. J Clin Invest 2006, 116:2610–2621
47. Benjamin LE, Golijanin D, Itin A, Pode D, Keshet E: Selective ablation of immature blood vessels in established human tumors follows vascular endothelial growth factor withdrawal. J Clin Invest 1999, 103:159–165
48. Hlushchuk R, Baum O, Gruber G, Wood J, Djonov V: The synergistic action of a VEGF-receptor tyrosine-kinase inhibitor and a sensitizing PDGF-receptor blocker depends upon the stage of vascular maturation. Microcirculation 2007, 14:813–825
49. Riesterer O, Honer M, Jochum W, Oehler C, Ametamey S, Pruschy M: Ionizing radiation antagonizes tumor hypoxia induced by antiangiogenic treatment. Clin Cancer Res 2006, 12:3518–3524